Fourteenth USA/Europe Air Traffic Management Research and Development Seminar (ATM2021)

Airport Ground Holding with Hierarchical Control Objectives

Christopher Chin*, Max Z. Li*, Karthik Gopalakrishnan, Hamsa Balakrishnan
Department of Aeronautics and Astronautics
Massachusetts Institute of Technology
Cambridge, MA, USA
{chychin, maxli, karthikg, hamsa}@mit.edu

***Abstract*—Disruptions in the air transportation system, perhaps due to extreme weather, often result in unexpected, or off-nominal, delays at airports. A resilient air traffic management system seeks to restore airport delays to their nominal values quickly after such disruptions. Two primary factors make the design of efficient recovery algorithms for air transportation networks challenging: the lack of a high-fidelity model for predicting and controlling airport delay dynamics, and poor computational tractability of large-scale flight rescheduling optimization problems. We propose a two-stage hierarchical control strategy for rescheduling aircraft (i.e., assigning delays) after network disruptions. Our high-level planner leverages a low-fidelity approximation of airport delay dynamics to propose a *reference plan* based on user preferences. This reference plan accounts for complex objectives such as ensuring a "smooth" redistribution of delays across airports (quantified by the total variation). The low-level controller then solves the multi-airport ground holding problem (MAGHP), augmented to track the reference plan. The solution to the augmented MAGHP yields a revised flight schedule with lower total variation than the original MAGHP, while still satisfying operational constraints. We illustrate the benefits of our proposed methodology using six disruption case studies of the National Airspace System (NAS).**

***Keywords*—flight delays; copula models; hierarchical control; traffic flow management**

I. Introduction

Air transportation is a critical infrastructure whose safe and efficient functioning is essential in the modern world. However, as with any large-scale system, disruptions and inefficiencies are also a part of the aviation infrastructure. Disruptions may be triggered by several factors, ranging from security and maintenance issues, airport equipment outages, or more commonly, poor weather. These disruptions result in reduced airport and airspace capacity, leading to demand-capacity imbalances. Such imbalances necessitate the implementation of traffic management initiatives (TMIs), resulting in flight delays, and in extreme cases, cancellations [1].

Flight delays and cancellations carry consequential, quantifiable costs for passengers, airlines, and the environment. In 2018, more than 2 million flights were delayed in the US alone, resulting in more than $30 billion in direct and indirect costs to passengers and airlines [2]. Swiftly recovering and restoring nominal performance after a disruption is critical. One of the key steps in system recovery is allocating limited airport and airspace sector capacity to the affected flights. Airport capacity is a critical bottleneck in the US National Airspace System (NAS), so we focus on airport capacities and delays in this paper [3]. Since every flight requires multiple resources in a sequential, coordinated fashion, identifying revised schedules that maximize resource utilization can be solved as an optimization problem. In this paper, we focus on the multi-airport ground holding problem (MAGHP), which is solved to allocate the limited landing and takeoff capacity at airports to disrupted flights [4], [5]. In particular, we propose an integrated data-driven control framework that *augments* the MAGHP with a reference plan determined by a high-level planner.

A. Motivation

The objective of the standard MAGHP is to minimize the total delay cost for the system while ensuring that airport capacity constraints are not violated. However, recent works suggest that minimizing the total system delays is a necessary, but not sufficient, criterion for recovery. For example, the spatial distribution of delays across airports has also been found to be an important measure of system disruption and recovery [6]. Unfortunately, incorporating the spatial distribution of delays into the MAGHP results in a computationally intractable optimization problem (Section III-B).

In this paper, we aim to develop a computationally scalable methodology that identifies flight schedules that not only minimize total system delay costs, but can also achieve other desirable objectives such as reducing the disparity in delays at airports, capping delays at specific airports, or even attempting to redistribute periods of peak delays to more favorable time slots. Our proposed methodology can be helpful to airlines in customizing their recovery process based on operational requirements. For example, an airline might want to protect its hub airports from high delays by transferring delays to other non-hub airports, perhaps with a small penalty in overall efficiency. Real-time decision support tools that mathematically capture and implement such preferences can facilitate robust recovery from disruptions.

* Authors contributed equally.

The NASA University Leadership Initiative (grant #80NSSC20M0163) provided funds to assist the authors with their research, but this article solely reflects the opinions and conclusions of its authors and not any NASA entity. The authors were also supported in part by NSF CPS Award No. 1739505. M. Z. Li was supported in part by a NSF fellowship.

B. Background and prior works

The MAGHP and its variants have been studied by several researchers [4], [5]. Prior works include analyzing solution sensitivity to delay [7] or sector utilization costs [8], and factoring in stochastic capacities [9]. Other extensions consider airline scheduling behaviors such as departure and arrival banks [10], as well as notions of fairness [11]–[13]. These studies primarily consider the magnitude of delays as a measure of system inefficiency and seek to minimize it. Recently, other aspects of system performance (e.g., spatial impact, fairness) have gained prominence. In [6], the authors examine spatial distributions of airport delays as an important attribute of the system from a network-wide and airline-specific perspective. In particular, *smooth* observations of airport delay signals, with respect to historical delay correlations, provide insights into disruption management and recovery. However, traditional MAGHP formulations are unable to tractably incorporate metrics that reflect spatial delay characteristics.

Air traffic management involves decision-making at multiple spatial and temporal scales [14]. For example, system disruptions and recoveries involve strategically planning hours into the future to allocate limited resources such as airport and airspace capacity. However, since disruptive events such as weather are often difficult to predict, these strategic measures are augmented with tactical actions by traffic flow managers and air traffic controllers, who assign reroutes or airborne holding [15]. As part of the Collaborative Decision-Making (CDM) process, airlines respond to these actions by swapping slots, aircraft, and crew; the goal is to minimize the impact of the evolving disruption on airline operations [16], [17]. Control of the air traffic management system at the sector-level or flow-level has been considered in previous studies [18]–[20]. Our approach adapts the idea of hierarchical controllers to incorporate objectives such as "smooth" delay distributions and customized airport recovery targets into the disruption-recovery process. We propose a layered control structure: A high-level layer that provides an unconstrained reference plan for NAS delays, which is then given to a low-level layer that constrains the plan to determine a flight schedule.

II. Problem Setup

Consider a set of flights scheduled to operate between a set of airports, all with known departure and arrival times. During disruptions, capacities at a subset of airports decrease, requiring some of these flights to be rescheduled. In this paper, we assume a time discretization of 15-minute intervals, in alignment with common on-time-performance metrics such as A14 [21]. The reduced capacities induce delays at airports, and we denote the delay (sum of departure and arrival delays) at airport i at time t as $x_i^{(t)}$. The vector of delays across all N airports indexed by $\{1,\dots,N\}$ at time t is denoted by $\mathbf{x}^{(t)} = \left(x_1^{(t)},\dots,x_N^{(t)}\right)^\top \in \mathbb{R}_{\geq 0}^{N\times 1}$. Denote by $\mathcal{T} = \{1,\dots,T\}$ the set of time indices, where $t \in \mathcal{T}$. With our hierarchical control framework, we seek to augment the standard MAGHP such that it is can provide schedule solutions incorporating goals such as: (1) Minimize $\sum_{i,t} x_i^{(t)}$, i.e., maximize efficiency; (2) Minimize $\sum_t \sum_{i,j} \rho_{ij} \left(x_i^{(t)} - x_j^{(t)}\right)^2$, i.e., maximizes delay signal smoothness with respect to network connectivity weights ρ_{ij}; (3) Achieve user-defined upper bounds on delays at targeted airports $\mathbf{x}^{(t)} \leq \mathbf{x}_{\max}^{(t)}$.

The notion of controlling airport delays via *redistribution* may be counter-intuitive, since delays are accrued quantities based on differences in scheduled versus actual arrival (or departure) times. This is in contrast to physical quantities (e.g., number of bikes at a bike-share station) where redistribution notions are more natural. To illustrate what we mean by redistributing airport delays, we provide the following example of how rescheduling flights can alter the delay vector $\mathbf{x}^{(t)}$ such that delays appear to have shifted from one airport to another.

Example: Let $f_{A\to C}$ and $f_{B\to C}$ be two flights from airports A and B to destination airport C, respectively, both with 2-hour flight times. Both $f_{A\to C}$ and $f_{B\to C}$ are scheduled to depart at 4:00 pm and arrive at C at 6:00 pm. Suppose that airport C can accept one aircraft at 6:00 pm and another aircraft at 6:15. This results in two possibilities: We can assign the 6:00 pm arrival slot to $f_{A\to C}$ (allowing it to depart as planned) and the 6:15 arrival slot to $f_{B\to C}$, or swap their orders. Note that both possibilities involve a 15-minute arrival delay at airport C (assuming no time is made up en route), but we have flexibility in determining whether airport A or B receives a departure delay of 15 minutes. This simple example depicts how airport delays can be redistributed per user preferences.

A. Challenges to be addressed

While incorporating efficiency and notions of airport delay smoothness within the standard MAGHP may seem straightforward, the resultant nonlinear optimization problem is computationally intractable at scale. Hence, our solution approach is to solve the problem in two stages. First, we identify a candidate reference plan for NAS delays at time t, denoted by $\mathbf{x}_\star^{(t)}$, that can incorporate a variety of user preferences, but has no knowledge of—and is unconstrained by—actual flight schedules. Next, we generate an actual feasible schedule by solving an augmented MAGHP with an additional objective term that attempts to track $\mathbf{x}_\star^{(t)}$ at each time step t. Our approach tackles two key challenges:

Challenge #1: Identifying a reference plan $\mathbf{x}_\star^{(t)}$ at each time t that can be realized by a feasible flight schedule requires a model for the system dynamics, which is often unavailable in such large-scale, stochastic, interconnected systems.

Challenge #2: Identifying a flight schedule that achieves some complex, possibly nonlinear, objectives may not be feasible through a standard implementation of MAGHP.

B. Solution framework

We present our hierarchical control framework in Fig. 1. The left-hand side of Fig. 1 provides an overview, wherein traffic flow management control actions are inputs into the NAS and result in observable performance metrics such as flight delays. Such real-time monitoring of the NAS has

become possible with initiatives such as System Wide Information Management (SWIM), the data-sharing backbone maintained by the FAA [22].

Our key contribution lies in the hierarchical design of the traffic flow management planning and control stages, i.e., the *high-level planner* and *low-level controller* blocks in Fig. 1, respectively. Out high-level planner, detailed in Section III-A), (1) provides a low-fidelity approximate model for the NAS state, as defined by the airport delays; and (2) allows for a wide range of user preferences in determining the NAS state evolution. In particular, the high-level planner can incorporate non-linear objectives (e.g., control the spatial distribution of delays or conditionally control delays at a subset of airports) and provide a reference plan for the NAS state in a computationally tractable manner. This addresses the first challenge we identified.

Our high-level planner incorporates some knowledge and assumptions regarding NAS delay dynamics (e.g., airport delays should be "continuous" across time), but it ignores the actual flight schedules and demands. While this enables computational tractability and application of customized user preferences, the high-level planner may provide a reference plan that is impossible for the low-level controller to exactly adhere to. Thus, to ensure that we generate a feasible schedule, we provide the high-level reference plan as a "weak" guidance to augment a low-level MAGHP controller. This approach is described in greater detail in Section III-B, and addresses the second challenge we identified. This hierarchical relationship between the high-level planner (more expressive, but potentially unrealistic) and low-level controller (more restrictive, but provides an actual adjusted schedule) forms the crux of our solution framework.

III. Methodology

A. High-level planner

Recall that our goal is to design a high-level planner that uses an approximate model for NAS delay states, combined with a design strategy, in order to propose a reference plan to be given to the low-level controller, the augmented MAGHP. Hence, we require realistic network delay state observations from some underlying probability distribution that describes the delay at each airport within the network. Two factors complicate this task: the marginal delay distributions at each airport may differ, and there could be a variety of dependencies between the delays at different airports. The former encapsulates the fact that different airports have significantly different operating characteristics (e.g., runway capacity, airspace structure, typical weather patterns), whereas the latter is the result of the networked nature of the system (e.g., tail-propagated delays, shared airspace constraints, traffic management initiatives).

To overcome both of these complicating factors, we use a statistical construct called a *copula*. A copula reparameterizes multivariate probability distributions, separating the tasks of estimating marginal distributions and estimating dependence structures [23]. Formally, an N-dimensional copula $C : [0,1]^N \to [0,1]$ is any valid cumulative distribution function $C(\mathbf{u}) = C(u_1, \ldots, u_N)$ with standard uniform random variables as its marginal distributions. The dependence between marginal distributions is completely captured by the functional form of C, whereas individual marginal distributions are represented by standard univariates $u_1, \ldots u_N$, after they are estimated and transformed via a probability integral transform. The advantage of using a copula lies in the fact that *any* continuous multivariate distribution can be uniquely represented by a copula. This fact is made precise by the following theorem:

Theorem 1 (Sklar's Theorem [24])**.** *Consider a N-dimensional cumulative distribution function $F_{\mathbf{X}}$ with marginals $F_{X_1}, \ldots, F_{X_N}$. Then, there exists a copula C such that $F_{\mathbf{X}}(x_1, \ldots, x_N) = C(F_{X_1}(x_1), \ldots, F_{X_N}(x_N))$ for all $x_i \in \mathbb{R}$ and $i = 1, \ldots, N$. Furthermore, if F_{X_i} is continuous for all $i = 1, \ldots, N$, then the copula C is unique.*

We can now estimate individual marginal airport delay distributions from data, and subsequently compute the copula C with a maximum likelihood estimator [25]. Finally, we note that a copula contains no temporal information, whereas airport delay distributions can be highly non-stationary [26]. While there are refinements such as time-varying *copula processes* [27], we capture the time-varying airport delay dynamics using 24 different copula models corresponding to each hour of the day.

Along with the copula-based approach for approximating NAS delay states, we use an approximate projection-based network control framework to construct the reference plan to be given to the low-level controller. In this paper, due to space limitations, we will only give an overview of this construction; for technical details, we refer the readers to [25]. To begin, we denote by $\mathbf{x}^{(t)} \in \mathbb{R}^N_{\geq 0}$ the vector of airport delays at time t. There are unknown system dynamics through which the airport delays evolve from time t to $t+1$. These dynamics are highly complex and unknown, necessitating the *approximate* and *low-dimensional* characteristics of this high-level planner.

Suppose we observe $\mathbf{x}^{(t)}$ and now would like to construct a reference plan for how airport delays should evolve at a high-level. Recall that the low-level controller (i.e., augmented MAGHP) is responsible for ensuring that a feasible schedule is produced; hence, instead of planning individual flights, we *project* $\mathbf{x}^{(t)}$ to a two-dimensional subspace of performance metrics, parameterized by the total delay and the *total variation* (TV) of the delays. Intuitively, the former measures the magnitude of delays, whereas the latter measures the spatial variance [6]. We can now set performance *targets* in the performance metrics subspace and construct a reference plan from candidate states within the approximate NAS delay distribution copula model.

Finally, we note that there may be multiple candidate states which satisfy our performance target. To select an *optimal* candidate state, we formulate the Conservative Selective Redistribution Problem (CSRP) in (1), an essential component of the high-level planner block in Fig. 1. In the CSRP formulation (1), $\widehat{\mathcal{X}} \subset \mathbb{R}^n$ denotes the copula-generated space of NAS delay states from which we find an optimal candidate $\mathbf{x}^{(t)}_\star \triangleq \mathbf{x}^{(t)}$ that minimizes a three-term objective, subject to

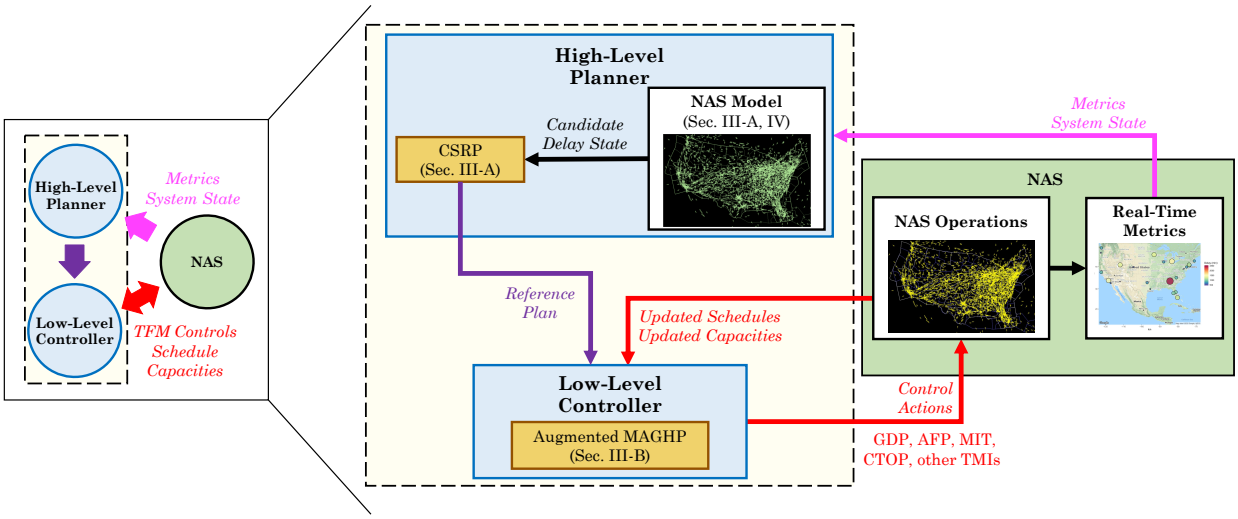

Figure 1: Representation of our hierarchical control framework.

a *delay conservation* constraint. We denote by $\lambda \in [0,1]$ the redistribution workload parameter; $\mathbf{c}$ a $N \times 1$ vector whose entry $c_i = 0$ for non-targeted airports, and $c_i = 1$ for targeted airports; $\left\{\mathbf{x}_B^{(t)}\right\}_{t=0}^{t=T}$ the set of baseline MAGHP airport delays; $\delta > 0$ a small tolerance factor, and $\mathbb{1}_N$ the $N \times 1$ vector where each entry is 1. The norms are standard ℓ_p-norms, i.e., $\|\mathbf{x}\|_\infty = \max_i |x_i|$ and $\|\mathbf{x}\|_1 = \sum_{i=1}^N |x_i|$. Formally, in the context of (1), the resultant reference plan from the high-level planner is the sequence $\mathbf{x}_B^{(0)} \cup \left\{\mathbf{x}_\star^{(t)}\right\}_{t=1}^{t=T}$.

$$
\begin{aligned}
\mathbf{x}_\star^{(t)} = \quad & \underset{\mathbf{x}^{(t)} \in \widehat{\mathcal{X}}}{\operatorname{argmin}} \left\{ \left\| \mathbf{x}^{(t)} - \mathbf{x}_\star^{(t-1)} \right\|_\infty + \lambda \tfrac{\mathbb{1}_N^\top \mathbf{c}}{N} \times \right. \\
& \left. \left\| \mathbf{x}^{(t)} - \mathbf{x}_B^{(t)} \right\|_\infty + (1-\lambda) \mathbf{c}^\top \left(\mathbf{x}^{(t)} - \mathbf{x}_B^{(t)} \right) \right\} \\
\text{s. t.} \quad & \left| \left\| \mathbf{x}^{(t)} \right\|_1 - \left\| \mathbf{x}_B^{(t)} \right\|_1 \right| \leq \delta, \\
& \mathbf{x}_\star^{(0)} = \mathbf{x}_B^{(0)}, \quad \lambda \in [0,1], \quad \forall t = 1, \ldots, T.
\end{aligned} \tag{1}
$$

The first term in the objective assesses a base penalty that enforces smooth transitions (i.e., delays are not "discontinuous") from the previous optimal candidate $\mathbf{x}_\star^{(t-1)}$. The second term elucidates why we refer to λ as a redistribution workload parameter: It interpolates between adherence to the baseline MAGHP solution (given by the second term) versus redistributing delays away from target airports (given by the third term). Note that since $\lambda \in [0,1]$, we must ensure that the second and third term are of comparable scales, so we introduce the normalizing constant $\mathbb{1}_N^\top \mathbf{c}/N$. This constant accounts for the fact that the third term is only evaluated over certain airports, whereas the second term is evaluated over every airport. Finally, the delay conservation constraint requires that all optimal state candidates have total delays that lie within a small δ-band of baseline MAGHP solution. For the case study results in Section V, we pick a δ-tolerance such that the CSRP remains feasible (i.e., there is a non-empty set of candidate states) while ensuring that the delay conservation constraints are enforced in practice.

B. Low-level controller

We consider an adapted version of the MAGHP. The mathematical notations used in the formulation are shown below.

A	:	set of all airports, indexed by i
F	:	set of all flights, indexed by f
$\mathcal{T}$	:	set of all time periods, indexed by t
F_{dep}	:	set of flights that depart in design day but arrive the next day
F_{arr}	:	set of flights that depart before the design day but arrive in design day
F_{full}	:	set of flights where we model the departure and arrival
F_d	:	set of flights where we model the departure
F_a	:	set of flights where we model the arrival
$dest_f$	:	destination of flight f
$orig_f$	:	origin of flight f
d_f	:	scheduled departure time of flight f
r_f	:	scheduled arrival time of flight f
T_{dep}	:	feasible departure times for flight f
T_{arr}	:	feasible arrival times for flight f
$D(i,t)$	:	departure capacity at airport i at time t
$A(i,t)$	:	arrival capacity at airport i at time t
v_{ft}	:	1 if flight f departs at time t, 0 otherwise
w_{ft}	:	1 if flight f arrives at time t, 0 otherwise

We have a set of flights F with scheduled and feasible departure or arrival times in $\mathcal{T}$ into airports $\mathcal{A}$. There are three main overlapping sets of flights that we use. $F_d = F_{dep} \cup F_{full}$ contains all flights where we model the departure. Likewise, $F_a = F_{arr} \cup F_{full}$ contains all flights where we model the arrival. F_{full} contains flights that depart and arrive within $\mathcal{T}$. Since demand exceeds airport capacity, we need to assign revised departure and arrival times to each flight, which are modeled with binary decision variables v_{ft} and w_{ft}, respectively. The following constraints must be satisfied:

$$\sum_{f \in F_d | orig_f = i, t \in T_f^{dep}} v_{ft} \leq D(i,t), \quad \forall t \in \mathcal{T}, i \in \mathcal{A} \quad (2a)$$

$$\sum_{f \in F_a | dest_f = i, t \in T_f^{arr}} w_{ft} \leq A(i,t), \quad \forall t \in \mathcal{T}, i \in \mathcal{A} \quad (2b)$$

$$\sum_{t \in T_f^{dep}} v_{ft} = 1, \quad \forall f \in F_d \quad (2c)$$

$$\sum_{t \in T_f^{arr}} w_{ft} = 1, \quad \forall f \in F_a \quad (2d)$$

$$\sum_{t \in T_f^{arr}} t w_{ft} - \sum_{t \in T_f^{dep}} t v_{ft} \geq l_f, \quad \forall f \in F_{full} \quad (2e)$$

Constraints (2a) and (2b) ensure that departure and arrival capacities are not exceeded across all airports and time periods. Constraints (2c) and (2d) require that all flights depart and land at some point within their feasible departure and arrival times. Note that in this implementation we do not consider connecting flights operated by the same aircraft, but this can be added in as additional constraints. Furthermore, the set of feasible arrival times T_f^{arr} and departure times T_f^{dep} for a flight f do not need to be fixed across time, allowing for adjustments due to, e.g., crew rest constraints. Finally, constraint (2e) ensures that the flight time for all flights is greater than or equal to their minimum travel time.

We now discuss the three models we use within the low-level controller. Note that constraints (2a)-(2e) apply across all models.

Baseline MAGHP: In the baseline MAGHP, the objective is to minimize *total delay cost* (TDC), which is a weighted sum of airborne delay and ground delay. The cost of one minute of airborne delay is c_a, which we assume to be 3, and the cost of one minute of ground delay is c_g, which we assume to be 1. The objective is formulated as follows:

$$\begin{aligned} TDC = {} & c_a \sum_{f \in F_a} \sum_{t \in T_f^{arr}} w_{ft}(t - r_f) \\ & + c_a \sum_{f \in F_{full}} \Big(\sum_{t \in T_f^{arr}} w_{ft}(t - r_f) - \sum_{t \in T_f^{dep}} v_{ft}(t - d_f) \Big) \\ & + c_g \sum_{f \in F_d} \sum_{t \in T_f^{dep}} v_{ft}(t - d_f) \end{aligned} \quad (3)$$

MAGHP with Redistribution (R-MAGHP): Suppose we have a set of target airports $\mathcal{A}_r \subset \mathcal{A}$ that we want to redistribute delay away from in time periods $\mathcal{T}_i^{redist} \subset \mathcal{T}$, where $i \in \mathcal{A}_r$. To encode this into the MAGHP, one option is to set maximum airport delay constraints for target airports at times of interest. But since such a formulation may be infeasible, this requires fine-tuning the maximum allowable delay at target airports. Instead, we formulate R-MAGHP by adding an additional penalty c_{at}^{target} to delay incurred at target airport $i \in \mathcal{A}_r$ across $t \in \mathcal{T}_i^{redist}$. For our case studies, we set $c_{at}^{target} = 1$ for all airports a and times t. The objective of R-MAGHP is to minimize TDC and the *target airport delay penalty* (TADP).

$$\begin{aligned} TADP = {} & \sum_{i \in \mathcal{A}_r} \sum_{\substack{f \in F_d \\ orig_f = i}} \sum_{\substack{t \in T_{dep}^f \\ d_f \in \mathcal{T}_i^{redist}}} c_{it}^{redist} v_{ft}(t - d_f) \\ & + \sum_{i \in \mathcal{A}_r} \sum_{\substack{f \in F_a \\ dest_f = i}} \sum_{\substack{t \in T_{arr}^f \\ r_f \in \mathcal{T}_i^{redist}}} c_{it}^{redist} w_{ft}(t - r_f) \end{aligned} \quad (4)$$

Augmented MAGHP (A-MAGHP): In addition to delay mitigation at target airports, suppose we would also like to control more complex delay behaviors such as its smoothness across a network of airports. The metric we use as a proxy for smoothness is TV, introduced in Section II. We first need the following equation for $x_i^{(t)}$, i.e., the delay at airport i at time t.

$$\begin{aligned} x_i^{(t)} = {} & \sum_{f \in F_d | orig_f = i, d_f = t} \sum_{t \in T_f^{dep}} v_{ft}(t - d_f) \\ & + \sum_{f \in F_a | dest_f = i, r_f = t} \sum_{t \in T_f^{arr}} w_{ft}(t - r_f) \end{aligned} \quad (5)$$

We define ρ_{ij} as the network connectivity weight between airports i and j. The intuition for TV is that minimizing TV encourages equalizing delay across airports with high network connectivity. Recall from Section II that $TV = \sum_{i,j|j>i} \rho_{ij} \sum_{t \in \mathcal{T}} \left(x_i^{(t)} - x_j^{(t)} \right)^2$. We can set our objective to be the sum of TDC and TV: Although we implemented and solved this for the MAGHP with up to 600 flights, it is difficult to solve for larger problems (e.g., 9,000+ flights) due to its non-linearity. Thus, we augment the MAGHP with a reference plan from the high-level planner by incorporating a linear tracking objective. Denote by $x_{\star,i}^{(t)}$ the delay at airport i at time t in the reference plan. Our new objective is to minimize TDC and the absolute deviation from the reference plan. Let $z_i^{(t)}$ denote the absolute deviation in total delay at airport i at time t relative to the reference plan. We ensure that $z_i^{(t)}$ can be encoded in a linear program with the following constraints: $z_i^{(t)} \geq x_i^{(t)} - x_{\star,i}^{(t)}$ and $z_i^{(t)} \geq x_{\star,i}^{(t)} - x_i^{(t)}$. The A-MAGHP objective is now to minimize TDC and the deviation from the reference plan ("reference deviation penalty", or RDP). The deviation penalty, i.e., the *tracking weight*, is denoted by $\theta \geq 0$.

$$RDP = \sum_{i \in \mathcal{A}_r} \sum_{t \in \mathcal{T}_i^{redist}} \theta z_i^{(t)} \quad (6)$$

Note that for both R-MAGHP and A-MAGHP, the redistribution penalties could be time-discounted to account for uncertainty in further out time horizons. This would apply to the penalties c_{at}^{target} in R-MAGHP and θ in A-MAGHP.

IV. Data Sources and Model Training

A. Airport capacities and schedule demand inputs

To compute the nominal and reduced arrival and departure airport capacities, we refer to the 2014 FAA Airport Capacity Profiles [28]. We illustrate our process of extracting 15-minute

arrival or departure airport capacities using Hartsfield-Jackson Atlanta International Airport (ATL) as an example. From [28], the arrival and departure capacity ranges between 168 to 226 aircraft per hour, dependent on weather conditions and configuration priorities, with an average capacity of 202 aircraft per hour. For ATL, the 15-minute nominal and reduced capacities are $\lfloor 202/4 \rfloor = 50$ and $\lfloor 168/4 \rfloor = 42$ aircraft, respectively. For the arrival capacities used in the MAGHP, we multiply the 15-minute capacities by a traffic fraction $\eta \in [0, 1]$ and an arrival fraction $\alpha \in [0, 1]$. Note that for departures, we perform the same calculation, except with a departure fraction $1 - \alpha$. Since our case study setups in Section V consider only the traffic between FAA Core 30 airports (i.e., origin and destination of all flights is an FAA Core 30 airport), the traffic fraction captures this fact by reducing the capacities in [28] accordingly. We also do not assume arrival or departure priorities, so we have that $\alpha = 1 - \alpha = 0.5$.

We construct the input flight schedule for our design day, i.e., the demand-side inputs of the MAGHP, based on origin-destination (OD) hourly traffic counts on August 5, 2019, retrieved from the Bureau of Transportation Statistics [29]. We map from hourly counts to a scheduled departure time by randomly assigning flights uniformly within four possible 15-minute windows for each hour. To account for the impact of overnight "red-eye" flights, our generated flights fall under three categories: (1) Flights with scheduled arrival and departure times within the 24-hour period (our design day); (2) flights departing prior to, and arriving within the design day; and (3) flights departing within, and arriving after the end of the design day. For scheduled arrival times, we sample from historical OD-specific normal distributions of flight times, retrieved from FAA ASPM [30]. The resultant flight schedule contains 9,838 flights, while the actual number of operated commercial flights in the FAA Core 30 airports on August 5, 2019 was around 13,600. The ratio between these two figures provides the aforementioned traffic fraction $\eta = 0.72$.

B. High-level planner model training

Recall from Section III-A that the high-level planner attempts to solve (1) at each time step $t = 1, \ldots, T$ in order to construct the reference plan $\mathbf{x}_B^{(0)} \cup \left\{ \mathbf{x}_\star^{(t)} \right\}_{t=1}^{t=T}$, where $\left\{ \mathbf{x}_\star^{(t)} \right\}_{t=1}^{t=T}$ are states residing within the copula-generated space of NAS delays $\widehat{\mathcal{X}}$. The high-level planner needs to be trained first on historical observations of NAS delays, so that $\widehat{\mathcal{X}}$ provides an adequate representation of NAS delays. We generate $M = 5419$ training samples $\left\{ \mathbf{x}_\ell^{(1)}, \ldots, \mathbf{x}_\ell^{(h)}, \ldots, \mathbf{x}_\ell^{(24)} \right\}_{\ell=1}^{\ell=M}$ containing delays at 30 airports across 24 hours, and use the subset of samples hour h to fit the multivariate Gaussian copula for hour h. For brevity, we direct the interested reader to [25] for the copula estimation procedure and other technical details.

Fixing the flight schedule generation procedure as described in Section IV-A, we generate the M training samples by solving a standard MAGHP, producing NAS delay vectors $\left\{ \mathbf{x}_\ell^{(1)}, \ldots, \mathbf{x}_\ell^{(h)}, \ldots, \mathbf{x}_\ell^{(24)} \right\}$ for the ℓ^{th} training sample. Since we want $\widehat{\mathcal{X}}$ to be as representative as possible in terms of NAS airport delays, we utilize a randomization-based heuristic (Algorithm 1) to explore and capture a wide range of possible airport delay conditions.

Algorithm 1 Randomization heuristic to perturb MAGHP airport capacity inputs.

Input: Flight schedule $\mathcal{D}$; Airports $\{1, \ldots, N\}$; Maximum, average, and minimum 15-minute capacities $\left\{ \mu_i^{\max}, \mu_i^{\text{avg}}, \mu_i^{\min} \right\}$ for each airport $i = 1, \ldots, N$; Maximum number of impacted airports $n_{\max} \leq N$; Low airport capacity tolerance $\gamma > 1$; Arrival fraction $\alpha \in [0, 1]$
Output: A training sample $\left\{ \mathbf{x}^{(1)}, \ldots, \mathbf{x}^{(24)} \right\}$

$n \leftarrow \mathcal{U}\{0, n_{\max}\}$
$\mathcal{A}_{\text{disrupt}} \leftarrow n$ airports uniformly at random from $\{1, \ldots, N\}$
for *Airport* $i \in \{1, \ldots, N\}$ **do**
  if $i \in \mathcal{A}_{\text{disrupt}}$ **then**
    Draw sample $c \overset{\text{iid}}{\sim} \mathcal{U}\left(\mu_i^{\min}, \min\left\{ \gamma \mu_i^{\min}, \frac{\mu_i^{\min} + \mu_i^{\text{avg}}}{2} \right\} \right)$
  else
    Draw sample $c \overset{\text{iid}}{\sim} \mathcal{N}\left(\mu_i^{\text{avg}}, \frac{\mu_i^{\max} - \mu_i^{\min}}{4} \right)$
  end
  $A(i, t) \leftarrow \alpha c, \forall t \in \mathcal{T}$; $D(i, t) \leftarrow (1 - \alpha) c, \forall t \in \mathcal{T}$
end
$\left\{ \mathbf{x}^{(1)}, \ldots, \mathbf{x}^{(24)} \right\} \leftarrow \text{MAGHP}\left(\mathcal{D}, \{A(i, t), D(i, t)\}_{i=1}^{i=N} \right)$

We note that the maximum, average, and minimum 15-minute capacities $\left\{ \mu_i^{\max}, \mu_i^{\text{avg}}, \mu_i^{\min} \right\}$ for each airport $i = 1, \ldots, N$ are retrieved in accordance with Section IV-A. For our case studies, we set $n_{\max} = 5$ airports and $\gamma = 1.2$. We denote a discrete uniform distribution between a and b by $\mathcal{U}\{a, b\}$, and its continuous analogue by $\mathcal{U}(a, b)$. The overall training procedure does not change for a real implementation of our framework: The MAGHP input would reflect all NAS flights (instead of flights only between FAA Core 30 airport), and accordingly, the training samples would simply be historical NAS delay observations (instead of multiple runs of MAGHP with perturbed capacities via Algorithm 1).

V. Case Study Results and Discussion

A. Disruption scenarios

We set up six different NAS disruption scenarios to test our hierarchical control strategy summarized in Section II-B. The first three disruption scenarios reflect reduced arrival and departure capacities at the top five hub airports by OAG connectivity index [31] for American Airlines (AA), Delta Airlines (DL), or United Air Lines (UA). The second set of three disruption scenarios detail reduced airport capacities within a specific geographic region. We list these disruption scenarios, along with the impacted airports, in Table I.

The airports in Table I have capacities set at $\mu_i^{\min}$, in contrast to the randomization heuristic in Algorithm 1 used to generate capacities at impacted airports. We remark that it is easy to replace these deterministic, constant capacities with time-varying capacities if such forecasts are available. We define user preferences to be the reduction of delays at *target* airports. For each scenario in Table I, we choose the five airports with the highest 15-minute delay in the baseline MAGHP solution as the target airports. We list

Scenario	Airports with Reduced Capacities
AA Hubs	CLT, DFW, LAX, PHL, PHX
DL Hubs	ATL, DTW, LGA, MSP, SLC
UA Hubs	DEN, EWR, IAD, IAH, ORD
Chicago	MDW, ORD
East Coast	BOS, BWI, DCA, EWR, IAD JFK, LGA, PHL
NYC	EWR, JFK, LGA

TABLE I. The six disruption scenarios and associated impacted airports.

these target airports in Table II. Note that the capacity-constrained airports in Table I are not necessarily the airports with the highest 15-minute delays. This is due to demand-side differences and varying severity of capacity reductions with respect to nominal capacities for different airports. Relating this back to the CSRP in (1), these preferences dictate that we prioritize delay mitigation at target airports within the high-level planner by setting $\lambda = 0$, such that the third penalty term $(1-\lambda)\mathbf{c}^\top \left(\mathbf{x}^{(t)} - \mathbf{x}_B^{(t)}\right)$ dominates.

Scenario	High-Level Planner Target Airports
AA Hubs	SFO, SEA, LAX, EWR, SAN
DL Hubs	BOS, IAD, SAN, SEA, SFO
UA Hubs	SFO, BOS, EWR, SEA, SAN
Chicago	SFO, SEA, SAN, ATL, BOS
East Coast	BOS, EWR, LGA, SAN, SFO
NYC	SFO, SEA, SAN, EWR, LGA

TABLE II. List of target airports for delay mitigation within the high-level planner.

B. AA Hubs scenario detailed results

We provide a deep dive into our hierarchical control framework applied to the "AA Hubs" disruption scenario. We compare three models: (1) a standard baseline MAGHP (Baseline), (2) MAGHP with redistribution (R-MAGHP), and (3) MAGHP augmented with a reference plan (A-MAGHP) given by a high-level planner focused on mitigating delay at target airports (see Table II). We highlight the various features of A-MAGHP and R-MAGHP for this disruption scenario. Throughout this subsection, we will also refer to the "AA Hubs" row of Table III for summary statistics of interest. We will discuss the remainder of the scenarios together in Section V-A, but only at the aggregate level of Table III.

Fig. 2 shows the projected hourly airport delays with the Baseline model for the "AA hubs" scenario. We first compare the total delay across the three models, shown in Fig. 3. Notice that the total delay of A-MAGHP tracks very closely with the Baseline, whereas R-MAGHP shows a sharp increase around 14:00 EDT, with somewhat lower delays in the following hours. R-MAGHP has the same total delay as the Baseline model, while A-MAGHP increases delay by a marginal 15 min. Both A-MAGHP and R-MAGHP successfully reduce delays at target airports: -13.2% and -18.1% with respect to the Baseline model, respectively. R-MAGHP provides larger delay reductions, at the price of more variability in airport delays, particularly around hours

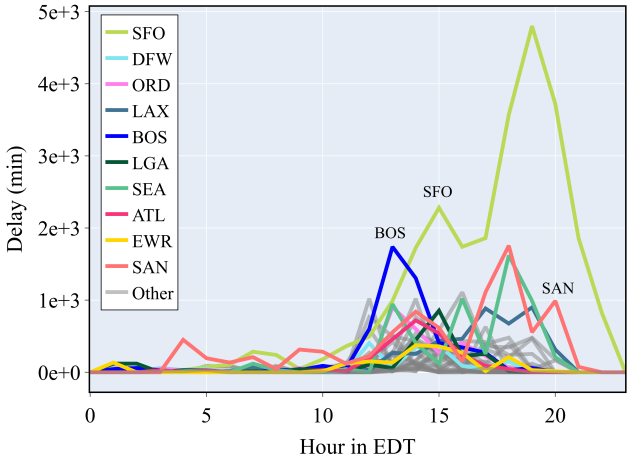

Figure 2: Airport delay time series corresponding to the solution of the Baseline model for the AA Hubs scenario.

14:00-16:00 EDT. The schedule from the R-MAGHP model may be more desirable if it is critical to mitigate delays at target airports, even at the cost of potentially large increases in delays at other airports, deviating significantly from the Baseline model. On the other hand, the A-MAGHP model schedule may be preferable to produce a "smoother" delay redistribution: one that prioritizes mitigation of delays at target airports, but also does not over-penalize non-target airports. This difference between delay impacts at target versus non-target airports can be visualized in Fig. 4, wherein we plot aggregate delays at target and non-target airports, across both R-MAGHP and A-MAGHP solutions. R-MAGHP results in a sharp spike in delay relative to Baseline for non-target airports at 14:00-15:00 EDT. This temporary spike contrasts with the more modest delay reduction relative to baseline at target airports. By contrast, with A-MAGHP the reductions in target airport delay more closely mirror the increases in non-target airport delay.

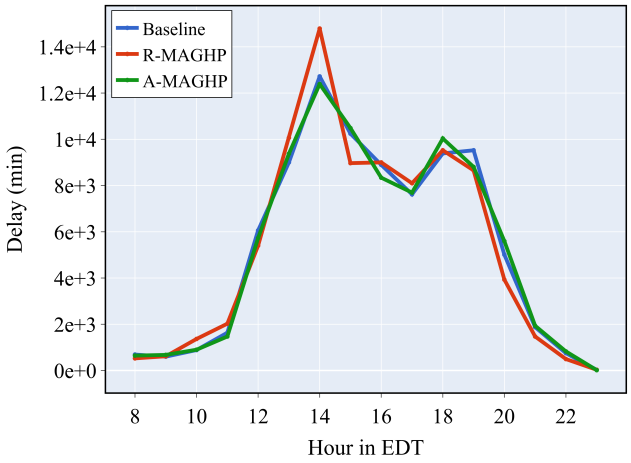

Figure 3: Total delay time series for the three models under the AA Hubs scenario. Early, low-delay hours are omitted for clarity.

We also plot in Fig. 5 individual OD pairs where the

departure (or arrival) times of flights were perturbed between the Baseline schedule and the schedule from the A-MAGHP model. We see that the OD pairs with higher percentages of perturbed flights tend to involve one of the target airports shown in blue, with an overall 13.2% reduction in delay at these target airports for A-MAGHP relative to baseline. Note that it is possible for the same OD pair to appear in both increasing and decreasing categories: suppose an OD pair had 10 flights, with 3 flights incurring increased delays in the A-MAGHP schedule compared to Baseline, and 4 flights incurring decreased delays. This would provide two different percentage increase (or decrease) values for this OD pair, as well as different average increase (or decrease) values.

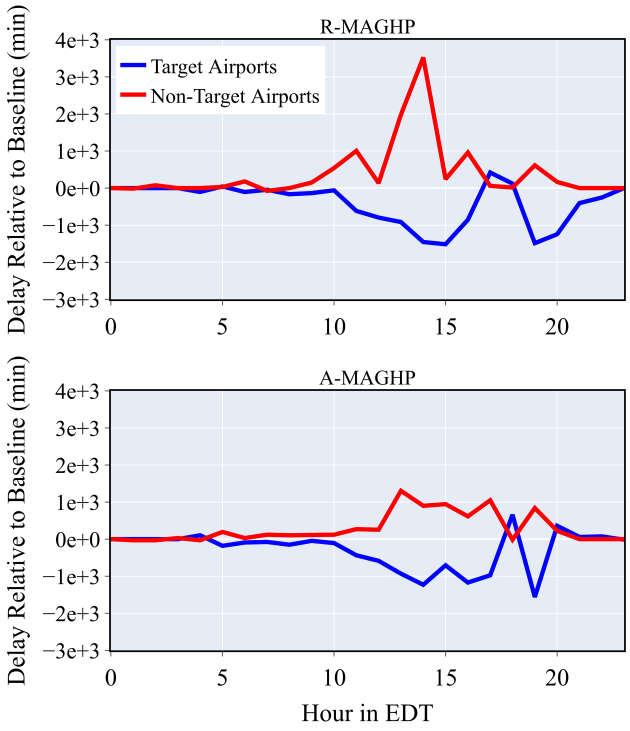

Figure 4: Change in delay between the Baseline model versus R-MAGHP and A-MAGHP, aggregated by target or non-target airports, for the AA Hubs scenario.

In terms of providing a revised schedule that minimizes TV, A-MAGHP outperforms R-MAGHP for the AA Hubs scenario, achieving -5.4% and -0.5% reductions compared to the Baseline, respectively. Fig. 6 shows the time series of TV across the three models. Recall from Section III-B that solving the MAGHP with explicit TV objectives is an intractable non-linear problem for our schedule containing 9,838 flights. By contrast, the hierarchical structure of A-MAGHP incorporates non-linear objectives by way of a linear tracking penalty based on a reference plan from the high-level controller.

We conclude our detailed analysis of the Baseline, R-MAGHP, and A-MAGHP results for the AA Hubs scenario by examining the impact of the tracking weight θ on the A-MAGHP schedule. In particular, we sample tracking weight values $\theta \in \{0.1, 0.2, \ldots, 1.2\}$, then plot in Fig. 7 the total delay and TV of each resultant schedule from A-MAGHP with

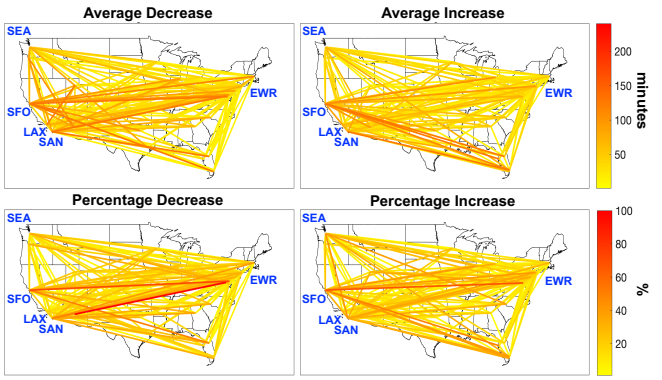

Figure 5: OD pairs plotted according to percentage of flights on that OD pair with decreased (or increased) delays, and the average delay decrease (or increase) in minutes, in the A-MAGHP model compared to Baseline. Target airports for delay mitigation for the AA Hubs scenario marked in blue.

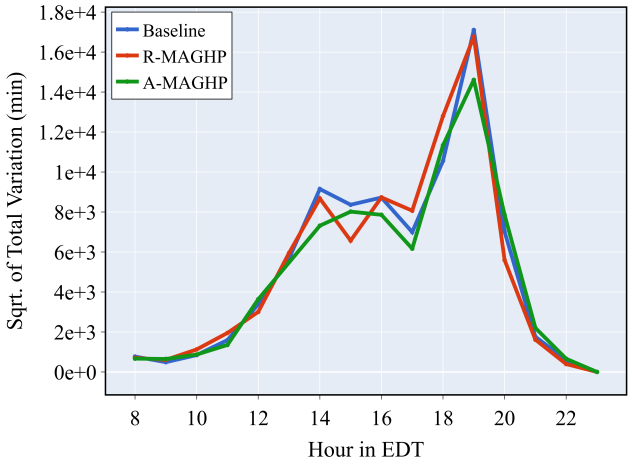

Figure 6: TV time series for the three models under the AA Hubs scenario. Early, low-delay hours are omitted for clarity.

different θ weights. We note that for this disruption scenario, the A-MAGHP outperforms Baseline and R-MAGHP in terms of TV with any of the sampled θ weights, but excessively large values of θ, i.e., $\theta = 1.2$ may result in higher delays with no additional TV improvements. Similarly, although picking smaller values of θ ensures that delays do not deviate from the Baseline model (in fact, A-MAGHP is equivalent to the Baseline for $\theta = 0$), benefits in terms of TV reductions may be lost. This provides a trade-off that can be explored by varying θ in the A-MAGHP formulation.

C. Summary of other scenarios

Table III provides a summary of the results of the Baseline, A-MAGHP, and R-MAGHP models across all six disruption scenarios. For A-MAGHP, the θ tracking weight is shown, which was chosen to minimize TV without a large increase in total delay. In terms of total delay, we see that R-MAGHP always resulted in delays identical to Baseline. Similarly, delays for A-MAGHP closely adhered to Baseline. For two disruption scenarios (AA Hubs and Chicago), A-MAGHP incurred no more than an additional 30 minutes of delay,

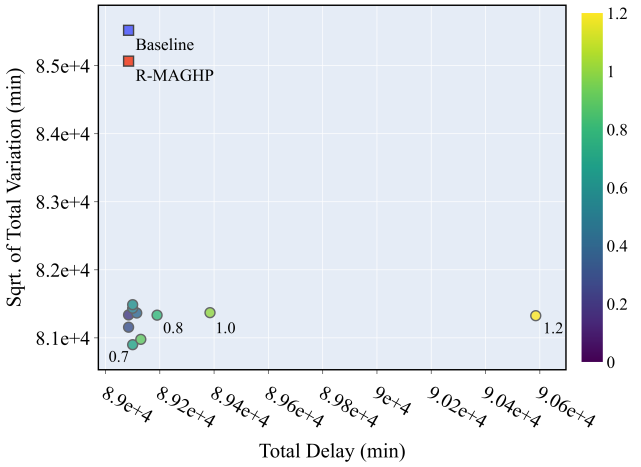

Figure 7: Effect of the tracking weight θ in the A-MAGHP model for the AA Hubs scenario.

across 30 airports and the 24-hour design day; for the other four disruption scenarios, A-MAGHP incurred no additional delay compared to Baseline. R-MAGHP, compared to A-MAGHP, results in a greater reduction in delay at target airports at the price of a greater increase in delay at non-target airports. Across all scenarios, A-MAGHP and R-MAGHP result in around 5-6% of flights experiencing a delay increase relative to Baseline and a similar percentage experiencing a delay decrease. The average increase (or decrease) in delays on a per-flight basis relative to Baseline is around 45-50 min.

In five of the six scenarios, A-MAGHP reduced TV significantly more (ranging from -5.4% to -9.3%) than R-MAGHP (ranging from -0.5% to -6.5%). The one exception is the East Coast scenario in which seven geographically correlated airports had reduced capacity. We note that our training data had at most five airports with reduced capacity, so it is possible that with more representative training of the high-level planner, the A-MAGHP's performance would improve. In a full-scale deployment of A-MAGHP, we would train using historical NAS airport delay observations, which would be more representative than the randomization heuristic in Algorithm 1. In addition, for the East Coast scenario, R-MAGHP is unable to significantly decrease TV. We hypothesize that it is inherently difficult to decrease TV in this scenario, with seven geographically clustered airports being simultaneously disrupted. Finally, we note that in practice, the schedule adjustments from A-MAGHP that result in delay transfers between airports depend on operational constraints (e.g., crew scheduling), coordination, and collaboration between airlines.

D. Potential feedback implementation

Thus far, we focused on how to generate a revised schedule for time horizon $t = 1, \ldots, T$ via the MAGHP augmented with a reference plan $\left\{\mathbf{x}_\star^{(t)}\right\}_{t=1}^{t=T}$. A real-time implementation with actual NAS metrics and system state would incorporate feedback in the form of updated airport capacities (e.g., airport updated weather forecasts) as well as updated schedules (e.g., some flights may have arrived or departed in conformance with the original schedule, but other flights may have been delayed). Suppose that at time $t = 0$, a schedule is produced by the MAGHP augmented with $\left\{\mathbf{x}_\star^{(t)}\right\}_{t=1}^{t=T}$. NAS operations begin according to this schedule, and the actual delay state $\widehat{\mathbf{x}}^{(1)}$ is observed at $t = 1$. Let $\Psi : \left(\widehat{\mathbf{x}}^{(1)}, \mathbf{x}_\star^{(1)}\right) \mapsto K$ be some *feedback mechanism* that examines the actual delay state $\widehat{\mathbf{x}}^{(1)}$ and the delay state projected by the reference plan $\mathbf{x}_\star^{(1)}$, then produces some feedback K that informs the generation of a new reference plan $\left\{\mathbf{x}_\star^{(t)}\right\}_{t=2}^{t=T}$ to augment the MAGHP from time $t = 2$ through the end of the time horizon. The specific form of the feedback K is flexible: Examples include (1) modifying the vector of target airports $\mathbf{c}$ in the CSRP; (2) adjusting the redistribution workload parameter λ in the CSRP; and (3) adjusting the tracking weight θ in the augmented MAGHP. Future work could involve designing such a feedback controller, using either real-time NAS data or a flight-level NAS simulator.

VI. Concluding Remarks

Motivated by the increasing ability to gather real-time NAS performance metrics and the question of designing new recovery pathways for NAS disruptions, we propose a hierarchical feedback control framework that incorporates a high-level planner (the CSRP) and a low-level controller (the MAGHP). The advantage of the high-level planner is its computational tractability and flexibility: users can input a wide range of preferences to the high-level planner, which then proposes a reference plan for NAS delays. This reference plan is then constrained by the low-level controller, the augmented MAGHP, which then produces a feasible flight schedule. We demonstrate the utility of this hierarchical framework using six NAS disruption scenarios. This control paradigm opens up a range of future work, from low-level controller refinements, such as adding flight connections or sector capacities, and incorporating other performance metrics such as flight cancellations.

References

[1] D. Bertsimas and S. S. Patterson, "The air traffic flow management problem with enroute capacities," *Operations Research*, vol. 46, no. 3, pp. 406–422, 1998.

[2] Federal Aviation Administration, Office of Aviation Policy and Plans, "Total cost of delay in the U.S. (2007-2019)," Federal Aviation Administration, Tech. Rep., 2020.

[3] D. Long, S. Hasan, V. L. Stouffer, K. Ramamoorthy, H. R. Idris, B. D. Ballard, and G. Carr, "Analytical identification and ranking of choke points in the national airspace system," in *15th AIAA Aviation Technology, Integration, and Operations Conference*, 2015.

[4] P. B. Vranas, D. J. Bertsimas, and A. R. Odoni, "The multi-airport ground-holding problem in air traffic control," *Operations Research*, vol. 42, no. 2, pp. 249–261, 1994.

[5] G. Andreatta and L. Brunetta, "Multiairport ground holding problem: A computational evaluation of exact algorithms," *Operations Research*, vol. 46, no. 1, pp. 57–64, 1998.

[6] M. Z. Li, K. Gopalakrishnan, K. Pantoja, and H. Balakrishnan, "Graph signal processing techniques for analyzing aviation disruptions," *Transportation Science*, 2021.

[7] M. Chaabouni, "Least-cost ground holding strategies with departure and arrival delay uncertainties," Master's thesis, Massachusetts Institute of Technology, 2 1999.

[8] Y. Xu, X. Prats, and D. Delahaye, "Synchronised demand-capacity balancing in collaborative air traffic flow management," *Transportation Research Part C: Emerging Technologies*, vol. 114, pp. 359–376, 2020.

Scenario	Model	θ	TD (min)	TD %Δ	$\sqrt{\text{TV}}$ (min)	$\sqrt{\text{TV}}$ %Δ	Delay %Δ Target	Delay %Δ Non-Target	% Flts Delay+	Avg Delay+ per Flt (min)	% Flts Delay-	Avg Delay- per Flt (min)
	Baseline	–	89,085	–	85,519	–	–	–	–	–	–	–
AA Hubs	A-MAGHP	0.7	89,100	0.017%	80,900	-5.4%	-13.2%	19.4%	5.7%	43.75	5.2%	-47.25
	R-MAGHP	–	89,085	0.000%	85,066	-0.5%	-18.1%	26.5%	5.3%	48.10	5.4%	-46.98
	Baseline	–	90,765	–	85,444	–	–	–	–	–	–	–
DL Hubs	A-MAGHP	0.4	90,765	0.000%	80,677	-5.6%	-9.6%	10.7%	5.5%	47.23	5.4%	-48.15
	R-MAGHP	–	90,765	0.000%	82,918	-3.0%	-14.7%	16.4%	5.3%	47.77	5.4%	-47.68
	Baseline	–	84,495	–	88,190	–	–	–	–	–	–	–
UA Hubs	A-MAGHP	0.6	84,495	0.000%	80,027	-9.3%	-9.2%	14.0%	5.4%	45.12	5.1%	-47.74
	R-MAGHP	–	84,495	0.000%	82,453	-6.5%	-13.3%	20.3%	5.1%	46.88	4.8%	-50.19
	Baseline	–	82,935	–	85,485	–	–	–	–	–	–	–
Chicago	A-MAGHP	0.9	82,965	0.036%	79,965	-6.5%	-8.6%	11.8%	5.1%	44.02	5.1%	-43.96
	R-MAGHP	–	82,935	0.000%	80,458	-5.9%	-14.5%	19.7%	5.3%	42.97	4.9%	-46.38
	Baseline	–	105,495	–	90,298	–	–	–	–	–	–	–
East Coast	A-MAGHP	0.5	105,495	0.000%	90,096	-0.2%	-5.6%	6.6%	6.1%	42.74	5.6%	-46.66
	R-MAGHP	–	105,495	0.000%	89,891	-0.5%	-6.4%	7.6%	6.0%	44.34	6.0%	-44.42
	Baseline	–	92,835	–	86,983	–	–	–	–	–	–	–
NYC	A-MAGHP	0.9	92,835	0.000%	81,364	-6.5%	-9.4%	13.0%	5.5%	45.63	5.4%	-46.78
	R-MAGHP	–	92,835	0.000%	82,310	-5.4%	-10.6%	14.6%	5.4%	47.26	5.4%	-46.45

TABLE III. Summary of results across all six disruption scenarios, comparing the baseline MAGHP, the augmented MAGHP (A-MAGHP), and the MAGHP with delay redistribution only (R-MAGHP). See Table II for list of target airports, and note that "+", "-" denote increasing and decreasing delays, respectively.

[9] O. Richetta and A. R. Odoni, "Solving optimally the static ground-holding policy problem in air traffic control," *Transportation Science*, vol. 27, no. 3, pp. 228–238, 1993.

[10] R. Hoffman and M. O. Ball, "A comparison of formulations for the single-airport ground-holding problem with banking constraints," *Operations Research*, vol. 48, no. 4, pp. 578–590, 2000.

[11] C. Barnhart, D. Bertsimas, C. Caramanis, and D. Fearing, "Equitable and efficient coordination in traffic flow management," *Transportation Science*, vol. 46, no. 2, pp. 262–280, 2012.

[12] D. Bertsimas and S. Gupta, "Fairness and collaboration in network air traffic flow management: An optimization approach," *Transportation Science*, vol. 50, no. 1, pp. 57–76, 2016.

[13] C. Chin, K. Gopalakrishnan, M. Egorov, A. Evans, and H. Balakrishnan, "Efficiency and fairness in unmanned air traffic flow management," *IEEE Transactions on Intelligent Transportation Systems*, pp. 1–13, 2021.

[14] A. Cook, *European air traffic management: principles, practice, and research*. Ashgate Publishing, Ltd., 2007.

[15] S. Grabbe, B. Sridhar, and A. Mukherjee, "Sequential traffic flow optimization with tactical flight control heuristics," *Journal of Guidance, Control, and Dynamics*, vol. 32, no. 3, pp. 810–820, 2009.

[16] T. W. M. Vossen and M. O. Ball, "Slot trading opportunities in collaborative ground delay programs," *Transportation Science*, vol. 40, no. 1, pp. 29–43, 2006.

[17] J. D. Petersen, G. Sölveling, J.-P. Clarke, E. L. Johnson, and S. Shebalov, "An optimization approach to airline integrated recovery," *Transportation Science*, vol. 46, no. 4, pp. 482–500, 2012.

[18] B. Sridhar and P. Menon, "Comparison of linear dynamic models for air traffic flow management," *IFAC Proceedings Volumes*, vol. 38, no. 1, pp. 13 – 18, 2005.

[19] P. K. Menon, G. D. Sweriduk, T. Lam, G. M. Diaz, and K. D. Bilimoria, "Computer-aided Eulerian air traffic flow modeling and predictive control," *Journal of Guidance, Control, and Dynamics*, vol. 29, no. 1, pp. 12–19, 2006.

[20] W. Chen and X. Hu, "Receding horizon control for airport capacity management," *IEEE Transactions on Control Systems Technology*, vol. 15, no. 6, pp. 1131–1136, 2007.

[21] "14 CFR, Part 234 - Airline Service Quality Performance Reports, Code of Federal Regulations," United States, 2016.

[22] Federal Aviation Administration (FAA), "SWIM Program Overview," Accessed 2021, https://www.faa.gov/air_traffic/technology/swim/overview/.

[23] R. B. Nelson, *An Introduction to Copulas*. New York, NY: Springer, 2006, pp. 7–49.

[24] A. Sklar, "Fonctions de répartition à n dimensions et leurs marges," *Publ. Inst. Statist. Univ. Paris*, vol. 8, pp. 229–231, 1959.

[25] M. Z. Li, K. Gopalakrishnan, and H. Balakrishnan, "Approximate projection-based control of networks," in *2020 59th IEEE Conference on Decision and Control (CDC)*, 2020, pp. 5573–5579.

[26] A. Jacquillat and A. R. Odoni, "An integrated scheduling and operations approach to airport congestion mitigation," *Operations Research*, vol. 63, no. 6, pp. 1390–1410, 2015.

[27] H. Manner and O. Reznikova, "A survey on time-varying copulas: Specification, simulations, and application," *Econometric Reviews*, vol. 31, no. 6, pp. 654–687, 2012.

[28] Federal Aviation Administration (FAA), "Airport capacity profiles (2014)," Accessed 2021, https://www.faa.gov/airports/planning_capacity/profiles/media/Airport-Capacity-Profiles-2014.pdf.

[29] US Department of Transportation, "Bureau of Transportation Statistics," 2019.

[30] Federal Aviation Administration (FAA), "Aviation System Performance Metrics (ASPM) website," 2018.

[31] Official Airline Guide (OAG), "Airport megahubs index 2019," Accessed 2021, https://www.oag.com/oag-megahubs-2019.

AUTHOR BIOGRAPHIES

Christopher Chin is a PhD Candidate in the Department of Aeronautics and Astronautics at the Massachusetts Institute of Technology. His research interests include optimization and protocols in air traffic management, including unmanned aircraft systems traffic management, as well as crew/airline scheduling.

Max Z. Li is a PhD Candidate in the Department of Aeronautics and Astronautics at the Massachusetts Institute of Technology. His research interests include air traffic flow management, aviation systems modeling, and applied mathematics, particularly geometric and topological methods.

Karthik Gopalakrishnan is a PhD Candidate in the Department of Aeronautics and Astronautics at the Massachusetts Institute of Technology. He is interested in the modeling, optimization, and control of air transportation networks.

Hamsa Balakrishnan is the William E. Leonhard (1940) Professor of Aeronautics and Astronautics at the Massachusetts Institute of Technology. Her research interests are in the design, analysis, and implementation of control and optimization algorithms for large-scale cyber-physical infrastructures, with an emphasis on air transportation systems. She is a recipient of the AACC Donald P. Eckman Award (2014), the AIAA Lawrence Sperry Award (2012), the CNA Award for Operational Analysis (2012), an NSF CAREER Award (2008), and several best paper awards in ICRAT and ATM Seminars.